

Integrated motor drive and non-isolated battery charger based on the split-phase PM motors for plug-in vehicles

Saeid Haghbin, Ola Carlson

Division of Electric Power Engineering, Chalmers University of Technology, SE-412 96 Gothenburg, Sweden
E-mail: saeid.haghbin@chalmers.se

Published in *The Journal of Engineering*; Received on 9th May 2014; Accepted on 20th May 2014

Abstract: A novel integrated motor drive and non-isolated battery charger based on a split-phase permanent magnet (PM) motor is presented and described for a plug-in vehicle. The motor windings are reconfigured by a relay for the traction and charging operation. In traction mode, the motor is like a normal three-phase motor, whereas in the charging mode, after windings reconnection, the system is a three-phase Boost rectifier. One important challenge to use the motor as three inductors in charger circuit is to have it in standstill during the battery charging. Based on the presented mathematical model of a split-phase PM motor, the zero-torque condition of the motor is explained which led to a proper windings reconnection for the charging. Simulation and experimental results of two separate practical systems are provided to verify the proposed integrated battery charger. Some practical limitations and design recommendations are provided to achieve a more realistic practical system.

1 Introduction

Batteries and battery chargers have a vital role on the development of more electric vehicles concept. The charger can be on-board or off-board. Moreover, it can be galvanically isolated or non-isolated from the utility grid. In addition, the charger power level is an important key factor that determines the charging time of the battery unit [1–3]. One way to classify the chargers is classification according to their power level. Table 1 shows a summary of the battery chargers according to the power level classification including the price range [3].

The ideal scenario for a vehicle user is to have a charger powerful enough to charge the battery in 5–10 min as is the case for refueling a normal car with an internal combustion engine. Moreover, they would like to have a good geographical coverage of the places that they can charge. It turns out that an on-board power level 3 is an ideal solution for customers that is not feasible at the moment because of price and volume of the charger (Table 1). Power level 2 chargers, i.e. semi-fast chargers, are a moderate solution compared with the slow and fast chargers that are available in the market today. An on-board semi-fast charger is a potential alternative in many types of plug-in vehicles like electric vehicles if the cost, volume and weight of the charger are within a reasonable range. As one can conclude from Table 1, for a semi-fast charger the price is still high enough to make it an expensive solution. In addition, those chargers are not small in volume. For example, for a liquid cooled high-power density battery charger with a power density of 1–2 kW/kg, a 20 kW charger weight is about 20–10 kg.

For plug-in vehicles, the traction circuit components including the electric motor, inverter and sensors are not engaged during the battery charging. Hence, there is a possibility to use them in the charger circuit to have an integrated motor drive and battery charger or simply an integrated charger. The traction circuit components for a passenger car are usually rated in a range of 50–100 kW that implies if one could utilise them in the charger circuit properly, there is a large potential to have a semi-fast charger yielding a considerable amount of savings in both the price and space. There have been different integrated motor drives and battery chargers, isolated and non-isolated, from both industry and academia that one can read a review and comparison in [1, 2, 4–14].

One of the main problems of using the traction motor in the charger circuit is developed torque in the motor because of current flow in the stator windings during the charging time. One

solution is to use a mechanical lock as is used in [14] or using an extra clutch and let the motor to run during the battery charging as is implemented in [13]. Another way of handling problem is to use a second inverter and control the developed torque to make it zero [7–9].

Split-phase electric motors have two similar stator windings that share the same magnetic circuit which can be shifted in the stator periphery. It is possible to connect the two sets of windings together and operate the motor by a single three-phase inverter for traction. If the motor windings connection are somehow changed for the charging, it is possible to cancel out the torque in the motor while there is a normal current flow in the motor. The main idea of this paper is to use a simple switching device like a relay to change the motor winding connection for the charging and traction mode. In the traction mode, the motor resembles a normal three-phase motor and in the charging mode, the developed torque is zero. Therefore there is no need for the second inverter or an extra clutch or a mechanical lock for the proposed solution. The proposed integrated charger is firstly presented in [1] which is extended in this paper by adding more analysis, simulations and practical measurements compared with the previous works [15]. Two different practical systems are constructed and tested with two different split-phase motors; one with a permanent magnet synchronous motor (PMSM) and another one with an interior PMSM (IPMSM). Based on the results of these two systems and their comparison, some design recommendations and practical limitations are provided.

Ideally, the charging power can be up to two times more than that of the traction power, but there are some practical limitations like bearing problem, audible noise and vibration that reduce the available power. Hence a finite element method (FEM) analysis is performed to quantify some of the limitations like developed torque. The main contributions of this paper can be summarised as:

- A non-isolated integrated motor drive and battery charger is explained in detail.
- The concept of motor zero-torque operation is presented and discussed.
- FEM results of the motor are provided to quantify the developed torque during battery charging.
- Some practical recommendations and limitations are provided.
- Practical results for two different setups are explained, one with a 20 kW IPMSM and another one with a 1 kW PMSM.

Table 1 Summary of the vehicle battery charger power levels including the price [3]

	Types	Source interfaces	Power levels	Approximate costs
level 1 120 V/230 V	on-board one-phase	normal plug	up to 3.5 kW	500–800 \$
level 2 230 V/400 V	on-board one- or three-phase	dedicated outlet	4–50 kW	1000–30 000 \$
level 3 480–600 V	off-board 3-phase	dedicated charger station	50–100 kW	30 000–160 000 \$

2 Mathematical model of a split-phase PM motor

In a two-pole three-phase PM motor, that can be a PMSM or an IPMSM type, there are three windings in the stator which are shifted 120 electrical degrees. In a split-phase PM motor, each phase winding is divided into two equivalent parts and are shifted symmetrically around the stator periphery. Basically, there will be six windings inside the stator, instead of three, for a two-pole machine.

The dynamic model of the electrical part of this machine can be described by the following equations as [13]

$$v_{d1} = r_s i_{d1} + \frac{d}{dt} \psi_{d1} - \omega_r \psi_{q1} \quad (1)$$

$$v_{q1} = r_s i_{q1} + \frac{d}{dt} \psi_{q1} + \omega_r \psi_{d1} \quad (2)$$

$$v_{d2} = r_s i_{d2} + \frac{d}{dt} \psi_{d2} - \omega_r \psi_{q2} \quad (3)$$

$$v_{q2} = r_s i_{q2} + \frac{d}{dt} \psi_{q2} + \omega_r \psi_{d2} \quad (4)$$

$$\psi_{d1} = L_d i_{d1} + L_{md} i_{d2} + \psi_{pm} \quad (5)$$

$$\psi_{q1} = L_q i_{q1} + L_{mq} i_{q2} \quad (6)$$

$$\psi_{d2} = L_{md} i_{d1} + L_d i_{d2} + \psi_{pm} \quad (7)$$

$$\psi_{q2} = L_{mq} i_{q1} + L_q i_{q2} \quad (8)$$

where L_d , L_q , L_{md} and L_{mq} are the direct and quadrature axis winding self and mutual inductances, respectively. The voltages, currents and fluxes in stationary rotor reference frame are presented by v , i and ψ with dq indices. It is assumed that the zero sequences are zero because of the symmetrical three-phase quantities. The developed electromagnetic torque can be expressed as

$$T_e = \frac{3}{2} \frac{P}{2} \left[\psi_{pm} (i_{q1} + i_{q2}) + (L_d - L_q) (i_{d1} i_{q1} + i_{d1} i_{q2} + i_{d2} i_{q1} + i_{d2} i_{q2}) \right] \quad (9)$$

For a PMSM with surface mounted magnets and a uniform airgap, $L_d = L_q$, so the developed electromagnetic torque simplifies to

$$T_e = \frac{3}{2} \frac{P}{2} \psi_{pm} (i_{q1} + i_{q2}) \quad (10)$$

The above torque equations are used to investigate the developed motor torque for different operations, the zero-torque condition for instance. For example, if two sets of currents are exactly the same but in opposite direction, then the developed torque is zero.

For the proposed integrated charger that is explained on the next section, the torque is zero in the charging mode because of opposite current flow in the stator windings considering the way that the motor windings are re-arranged.

3 Non-isolated battery charger based on the split-phase PM motor and a switching relay

The power stage of a traction system based on an AC motor and a three-phase inverter is shown in Fig. 1. In several schemes a DC/DC converter is used between the battery and inverter [16] which is not the case here. The main available components that can be used in the charger circuits are the inverter including the DC bus capacitor, AC motor as inductors, measurement sensors (usually phase currents and DC bus voltage) and the controller. As mentioned earlier, the main challenge of using the motor as inductors is keeping the torque zero during the battery charging; otherwise the vehicle may run away during the battery charging.

Fig. 2 shows the proposed motor drive and non-isolated battery charger based on the split-phase PM motor. Without lack of generality, the motor is a split-phase PM motor with an arbitrary phase-shift between two sets of three-phase windings. Moreover, the midpoints of the motor windings for each phase are available. The system in traction, charging and the physical realisation are shown in this figure. A simple switching device is used to reconfigure the system for the traction to charging and vice versa.

The resulted circuit topology in charging mode is a three-phase Boost rectifier which is explained later on. In traction mode, the system is like a normal three-phase AC drive, so it is not explained here further.

In charging mode the electric motor can handle the current two times more than that of the traction mode because of the parallel winding connection. It is possible to connect the motor windings in series as is presented in [1]. Consequently, the charging power can be increased twice compared with this scheme, if the inverter could handle that. However, the total leakage inductance in this case is lower than in the first case meaning that the current ripple is higher. To be more specific, if the total inductance per phase is $2L_r$ for the series winding connection, the total leakage inductance per phase is $L_r/2$ for parallel connection (Fig. 2) that is four times lower.

Unity power factor operation is one feature of this charger. However, the main limitation of the rectifier in this topology is that the output DC voltage should be more than the peak line voltage to have unity power factor operation. Additionally, there might be a need to add a small line filter to meet the total harmonic distortion (THD) requirements [17] during the battery charging operation. Another advantage of the circuit is bidirectional operation capability. Hence, it is possible to use the device for G2V applications.

As is shown in Fig. 2, just a simple switch is needed to reconfigure the traction circuit to the charging circuit. Moreover, both three-phase and single-phase supplies can be connected to the circuit

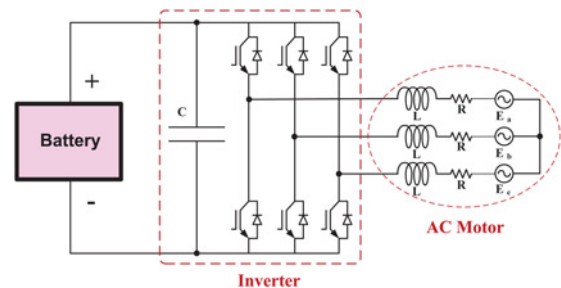


Fig. 1 Power stage of a traction circuit based on a three-phase motor and an inverter

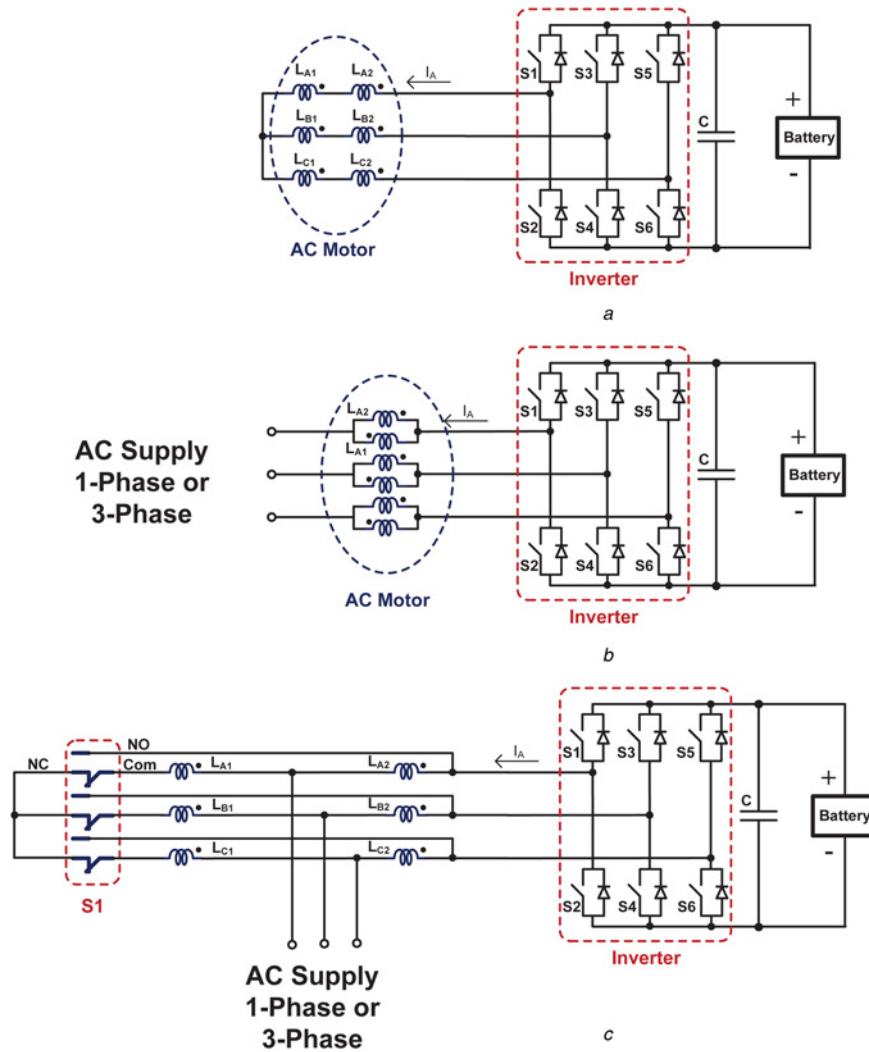


Fig. 2 Non-isolated integrated motor drive and battery charger based on the split-phase PM motor and a switching device
a System in traction mode
b System in charging mode
c Hardware realisation for the traction or charging

without any changes in the hardware in charging mode. However, there are some changes in the control algorithm for this purpose.

The motor torque is calculated by using (9) for the split-phase PM motor. If the system is supplied by a symmetrical three-phase source and the motor has ideally sinusoidally distributed windings and induced magnet flux, then the resulted torque is zero for the charging mode [1].

4 Three-phase Boost battery charger

There are different circuit topologies for the grid-connected battery chargers [18, 19] which the three-phase Boost rectifier is one of the well-known schemes enabling high-power charging. Fig. 3 shows a basic diagram of this converter which the proposed non-isolated integrated charger is based on this circuit topology. As mentioned earlier, the motor is used as three inductors by a proper winding's re-arrangement.

The voltage equations describing the converter in the dq reference frame are as [20]

$$u_{Ld} = Ri_{Ld} + L \frac{d}{dt} i_{Ld} - \omega Li_{Lq} + u_{ld} \quad (11)$$

$$u_{Lq} = Ri_{Lq} + L \frac{d}{dt} i_{Lq} + \omega Li_{Ld} + u_{lq} \quad (12)$$

where u_{Ld} , u_{Lq} , u_{ld} and u_{lq} are the line and inverter dq voltage components, respectively, whereas R , L and ω are the resistance, inductance and source frequency, respectively, and i_{Ld} and i_{Lq} are the d and q components of the line currents, respectively [21, 22]. The converter active power, p , can be written as [20]

$$p = \frac{3}{2} (u_{Ld} i_{Ld} + u_{Lq} i_{Lq}) \quad (13)$$

Based on the system equations and presented controller, MATLAB/

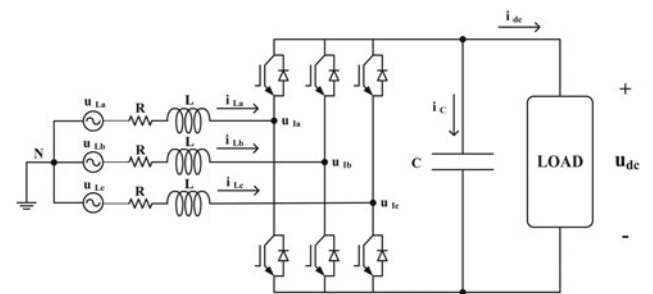


Fig. 3 Power stage of the three-phase Boost converter

Table 2 Parameters of the three-phase Boost converter

Parameters	Values
power	15 kW
input voltage	400 Vac, three-phase
DC bus voltage	700 Vdc
DC bus capacitance (C)	100 μ F
inductance (L)	3 mH
resistance (R)	0.10 Ω
switching frequency	10 kHz

SIMULINK package is used to simulate a three-phase Boost rectifier with a power level of 15 kW. The rectifier parameters are presented in Table 2. Fig. 4 shows the simulation results for a step change of the load from 15 to 7.5 kW. Three-phase line currents, voltages and DC bus voltages are shown in this figure. Moreover, phase A voltage and current are presented in a same plot to show the unity power factor operation where the detailed control design is explained in [21]. The inductance value, L , is 3 mH that is a typical value for these applications. The motor leakage inductance used in the proposed charger is in the same range. However, one needs to adjust the control parameters like the switching frequency according to the available motor inductance in the charging mode.

5 Two practical systems for the proposed non-isolated integrated charger

To practically verify the proposed integrated charger, two experimental systems have been developed based on the two different PM motors: (i) a 20 kW split-phase multi-barrier IPM motor with two sets of three-phase windings that have a $\pi/6$ degree shift in the stator periphery and (ii) a 1 kW PMSM with double stator windings with two sets of three-phase windings which are not shifted and are identical.

The FEM analysis has been performed for the 20 kW motor to have more accurate results to encounter the motor winding harmonics. In addition, some practical limitations have been detected that

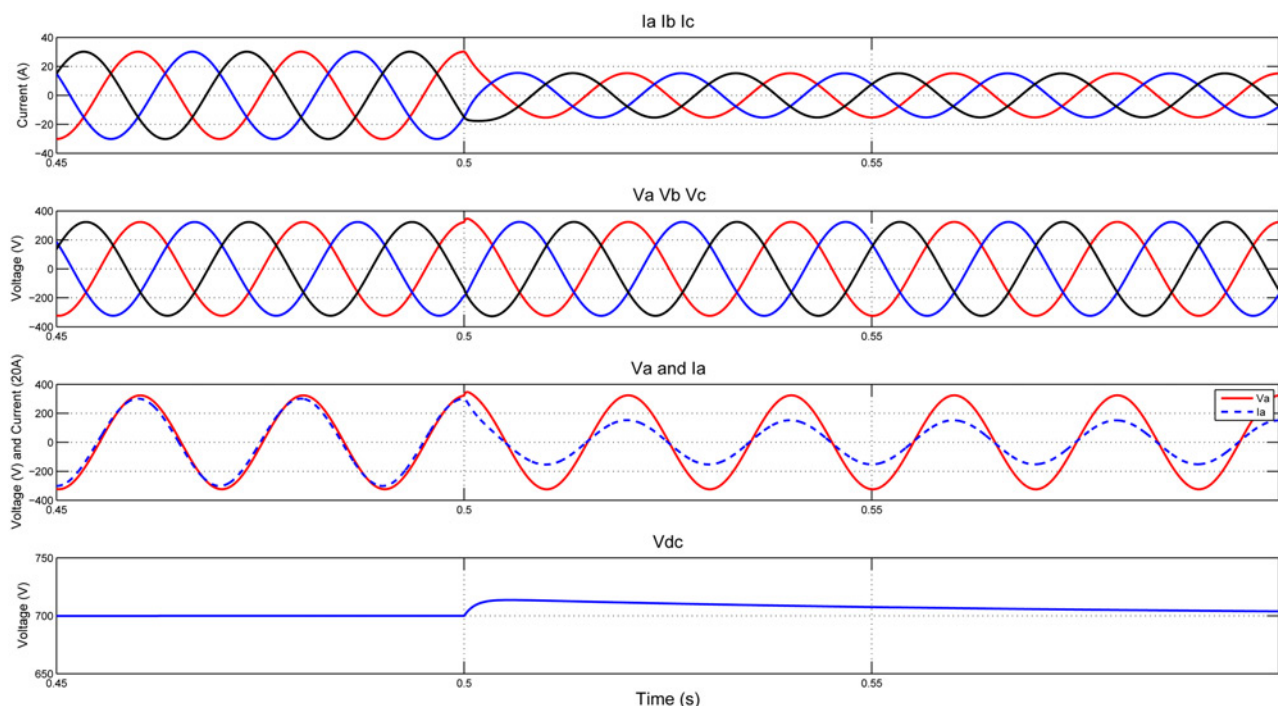
give more insights for implementation considering the vehicle application.

5.1 Practical system 1: proposed non-isolated integrated charger based on a 20 kW IPM motor

A 20 kW PM motor is designed and implemented for an isolated integrated charger explained in [13]. A non-isolated version of the battery charger is implemented based on the scheme explained in the previous section. Winding configuration, FEM simulation results, MATLAB simulation results and practical measurements show that the proposed scheme is practically feasible.

Fig. 5 shows the proposed system in traction and charging modes for the 20 kW PM motor in which the parameters are presented in Table 3 [13]. However, for this PM motor, because of winding's space harmonics, the maximum current in each winding is measured to be half of the rated value before reaching a high-level audible noise. Therefore a maximum total current of 15 A_{rms} is permissible for the battery charging that is equivalent to a power level of 10 kW. As is explained later on, the motor audible noise is the main limitation to increase the battery charging power level for this motor. The motor is a water cooled four pole IPMSM machine that is designed and optimised for the vehicle traction application. As long as the zero-torque condition can be held in the motor during the charge operation, it is possible to use the split-phase PM motor inductances in the charger circuit. If the same current is flowing into the two sets of windings with opposite directions, the developed torque is ideally zero. However, because of the windings harmonic contents or variable rotor position dependent phase inductances, there is a winding's current limitation that reduces the maximum charge power. In this case, by reducing the charge power, one can reach an acceptable level of power for the battery charging.

(1) *FEM simulation results for the 20 kW IPM motor:* Ansoft/Maxwell software package is used to perform simulations for the motor during battery charging. A symmetrical three-phase sinusoidal current with a peak value of 9 A and a frequency of 50 Hz is assumed for the motor. Simulation has been conducted for the

**Fig. 4** Simulation results: three-phase Boost rectifier with a step load change

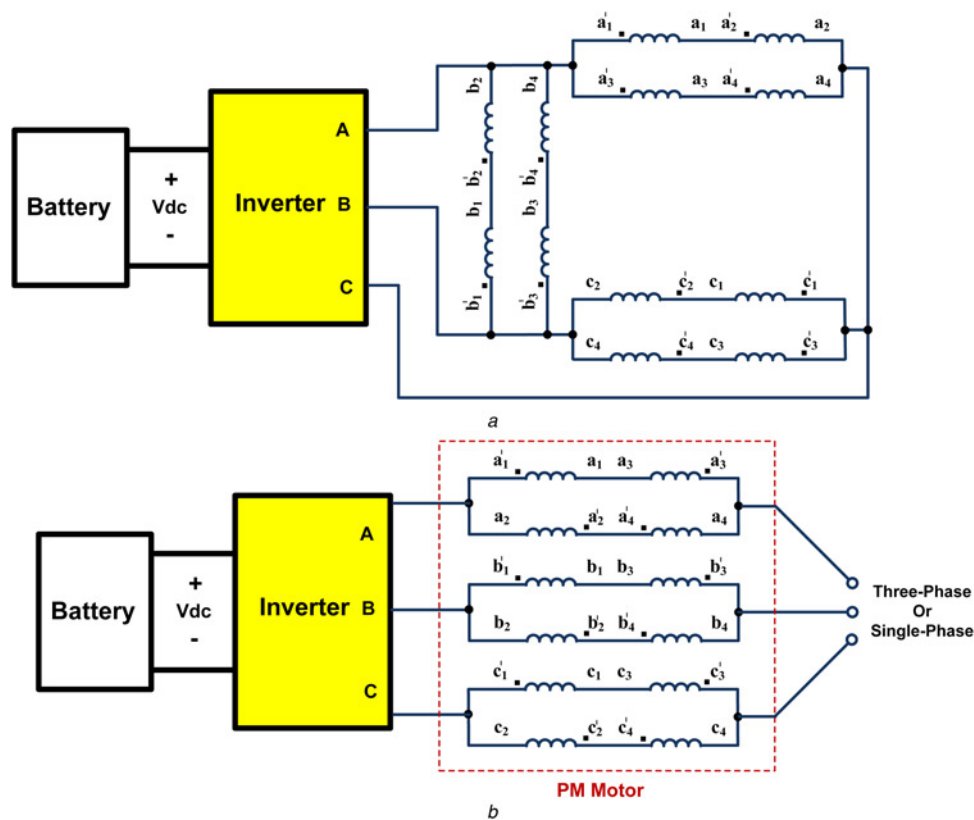


Fig. 5 Non-isolated integrated charger based on the split-phase 20 kW PM motor with the parallel connected windings
a Traction
b Charging

different rotor positions while the motor is in standstill. Fig. 6 shows the basic geometry and magnetic field distribution for the time instant that the phase A current is in the maximum value ($t = 5$ ms). As is shown in the figure, the motor laminations are exposed to a variable flux density. Consequently, there is a magnetic core loss in laminations during the battery charging. However, ideally, the flux variation is close to zero and iron loss shall be negligible. The mutual flux in the motor is zero with the proposed winding arrangement; assume that two sets of identical windings magnetise a common core with opposite current directions. In this case, the leakage inductance is used as the energy storage device which does not contribute in torque development.

The inductance of an IPM motor varies as a function of the rotor position. Subsequently, the inductance and torque depend on the rotor position during the charge operation. The rotor is in standstill but it can be in any position. Figs. 7 and 8 show the motor phase A inductance and the developed electromagnetic torque for different

rotor positions. For a three-phase Boost converter, the inverter controls the motor currents, so the inductance variation is not critical and a proper control operation can reduce the adverse impact. Compared with the nominal torque that is 127 Nm, the developed torque is small. Fig. 8 shows the motor torque for different rotor positions. As is shown in the figure the developed torque is $< 3\%$

Table 3 20 kW IPM motor parameters

	Values	Units
rated power	20	kW
rated speed	1500	r/min
number of poles	4	—
permanent magnet flux	0.27	Wb
stator resistance	0.3	Ω
d -axis inductance	14.9	mH
q -axis inductance	39.9	mH
inertia	0.04	kg m^2
viscous friction coefficient	0.01	Nm s/rad

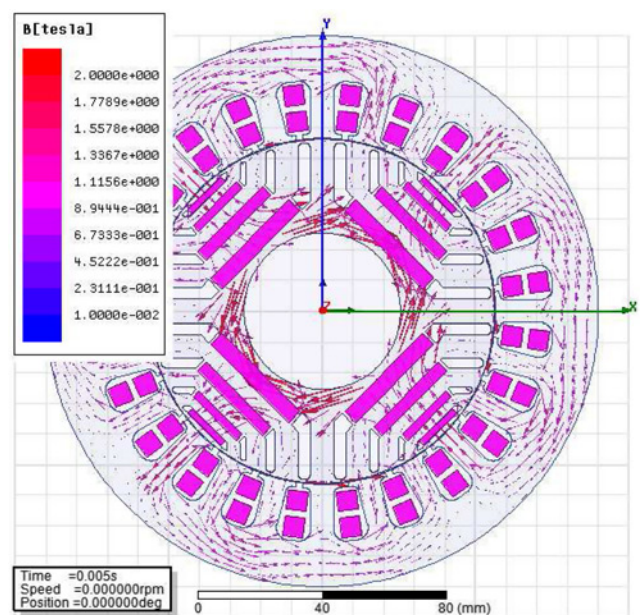


Fig. 6 Simulation result: magnetic flux density distribution in the 20 kW IPMSM during battery charging in non-isolated integrated charger

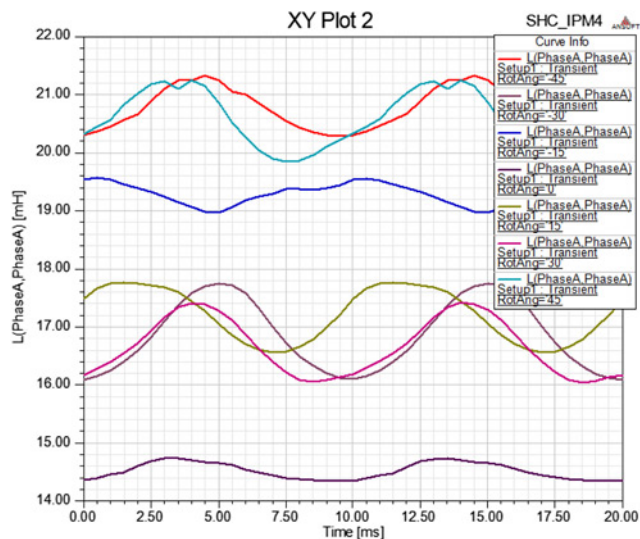


Fig. 7 Simulation result: phase inductance in the 20 kW PM motor during battery charging for different rotor positions

of the rated torque. Moreover, the average torque is close to zero which means the motor will be in standstill during charging. As is explained later on with experimental results, there is an audible noise when the magnitude of the current and resulted torque is high. As mentioned earlier, for this motor when the current is more than half of the rated value, the motor starts to sound.

For a three-phase rectifier, the value of inductor cannot be too low or too high. The first one causes a large THD value and the second one makes the control difficult because of the large voltage drop on the inductor. By connecting the motor windings in series or parallel, designer has the option to select the inductor value that is close to the desirable one. However, there are other parameters in the system, like switching frequency, that will impose other constraints on the charger.

(2) *Practical system results for the 20 kW IPM motor:* To verify this non-isolated integrated charger, a simple practical system is developed which the motor is used as three inductors in which Fig. 9 shows the system configuration. The three-phase or single-phase

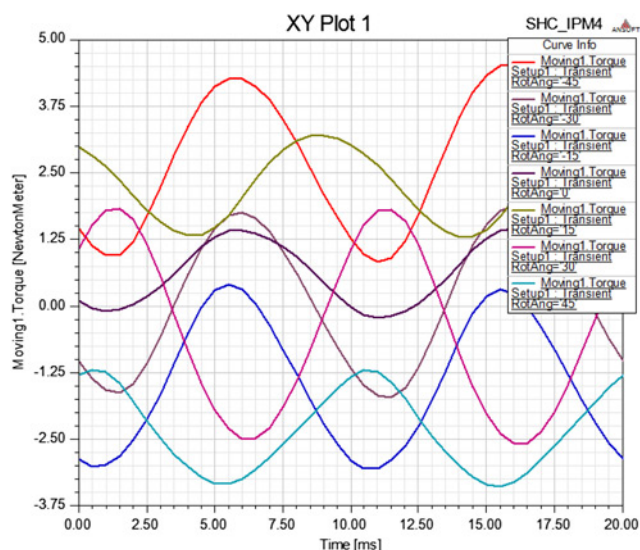


Fig. 8 Simulation result: developed torque in the 20 kW PM motor during battery charging for different rotor positions

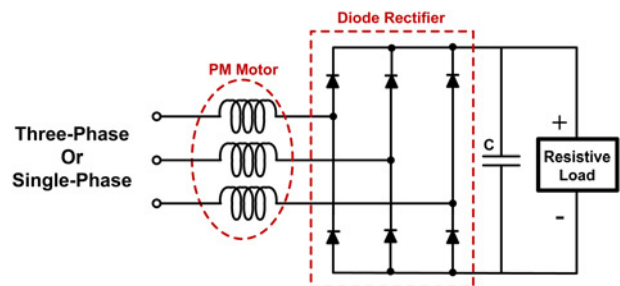


Fig. 9 Main diagram of the practical setup for the 20 kW PM motor

supply is connected to the motor that is connected to a diode bridge rectifier. A large capacitor, 3300 μ F, reduces the ripple on the DC bus. The motor behaviour, like audible noise and waveforms, are studied in this setup.

This bridge rectifier is a naturally commutated rectifier that one can find detailed explanations in classical power electronics textbooks [23]. Fig. 10 shows the measured supply voltage, line (motor) current and motor voltage. As is shown in this figure, the waveforms are heavily distorted because of the grid frequency rectification and diode rectifier operation. To calculate the motor phase inductance, the root-mean-square values of the motor's voltage and current are calculated by use of the measured and recorded data. The calculated value of the inductance is 7 mH that is lower than the simulated value in FEM (see Fig. 7). However, the calculated value using the measurement data is based on the assumption that the voltages and currents are pure sinusoidal.

The rectifier system is simulated in MATLAB/SIMULINK using Power System Blockset. The measured value of the inductance, 7 mH, is used in this simulation. Fig. 11 shows one-phase of the motor current and voltage for both the measurement and MATLAB simulation. The current waveforms are very similar, but for the voltage there is a difference. The inductor voltage is the derivative of the current that is a noisy operation that can be one reason of the difference in addition to winding's space harmonics.

5.2 Practical system 2: proposed non-isolated integrated charger based on a 1 kW PMSM motor

As the second example, a practical setup is designed and implemented based on a 1 kW split-phase PMSM. Fig. 12 shows a basic diagram of the motor cross-section area. An available PMSM is re-winded to have two identical sets of three-phase windings that are not shifted in stator periphery. The motor is not optimised for this application. Nevertheless, it is possible to verify the system

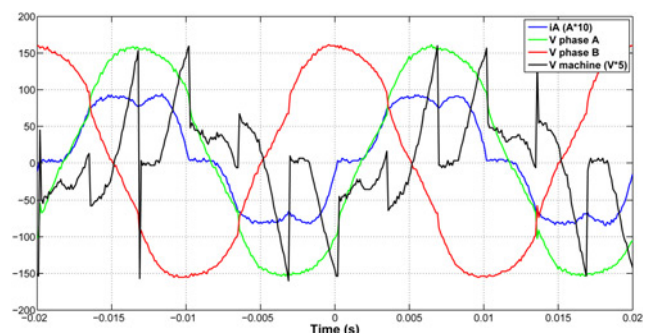


Fig. 10 Measurement: supply voltage and motor waveforms of non-isolated integrated charger in the bridge rectifier setup; the voltages are in V and currents are in A

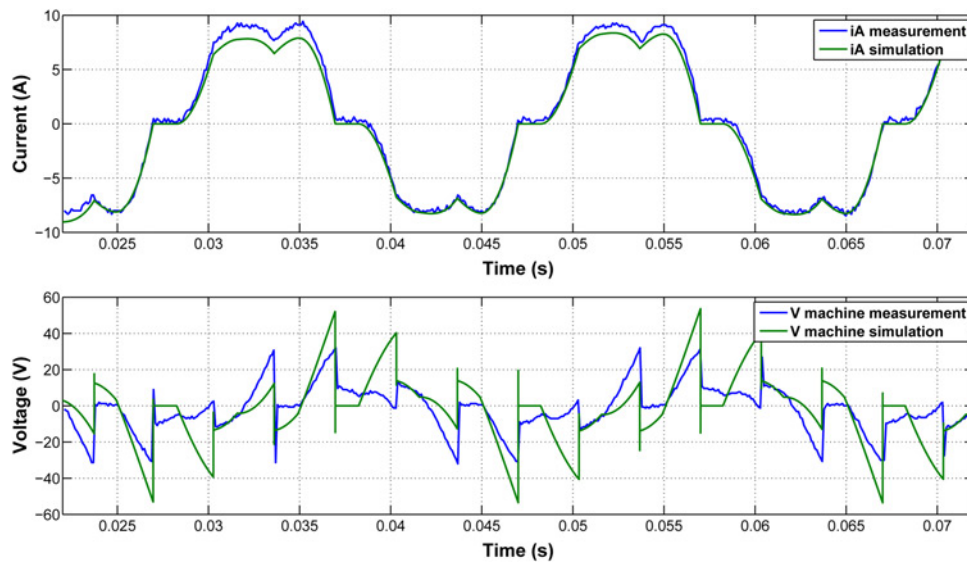


Fig. 11 Measurement and simulation: measurement and MATLAB simulation of the motor phase voltage and current of non-isolated integrated charger in the bridge rectifier setup

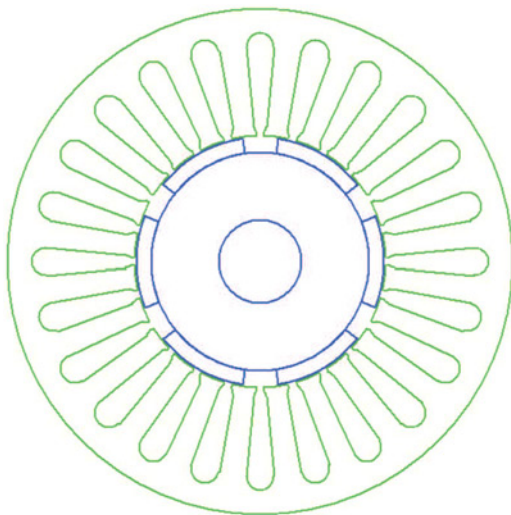


Fig. 12 Cross-section diagram of the 1 kW PMSM motor

functionality with this setup. Fig. 13 shows the system configuration in charging mode, and the motor parameters are presented in Table 4.

(1) *CompactRIO implementation of the 1 kW system*: A control system based on the CompactRIO platform is developed for the control, voltage-oriented control, of integrated charger that is a Boost rectifier now. Fig. 14 shows the main diagram of the experimental system based on the CompactRIO platform. This setup includes: an inverter, the motor as three inductors, isolated current measurement modules, isolated voltage transducers, a load and the CompactRIO control system.

The CompactRIO platform includes I/O modules, a reconfigurable FPGA and an embedded controller (processor). The whole control is divided between the FPGA board and the embedded controller. FPGA is responsible for the data acquisition, calculation of the grid voltage phase by a software-based phased locked loop (PLL) and the PWM generation. The dq transformation and other control actions like current controller and feedforward compensations are performed in the processor.

The above explained experimental setup is tested for the charging mode with an AC supply voltage of $75 V_{LL}$ and a 200 W charging power. The controller is set to maintain a constant DC voltage in the DC bus that is 100 V with a nominal DC current of 2 A. The value of i_q is set to zero in the control stage to achieve a unity power factor operation. Fig. 15 shows the phase A voltage and current of the AC supply line. During the charge operation, the voltage drop in the

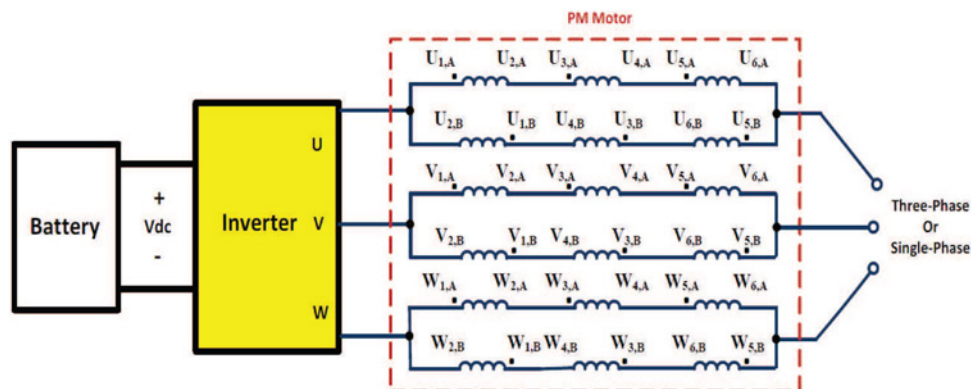


Fig. 13 Non-isolated integrated charger based on the 1 kW PMSM motor with double windings

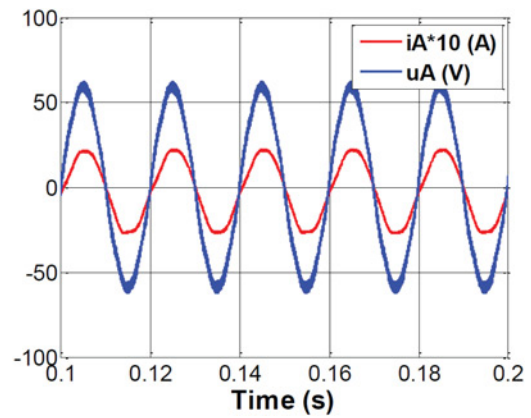
Table 4 1 kW PMSM motor parameters for the battery charging

	Values	Units
rated power	1	kW
rated torque	3.9	Nm
rated speed	1000	r/min
number of poles	6	—
number of slots	24	—
airgap length	0.5	mm
winding type	distributed	—
stator resistance	3.57	Ω
leakage inductance	4.64	mH

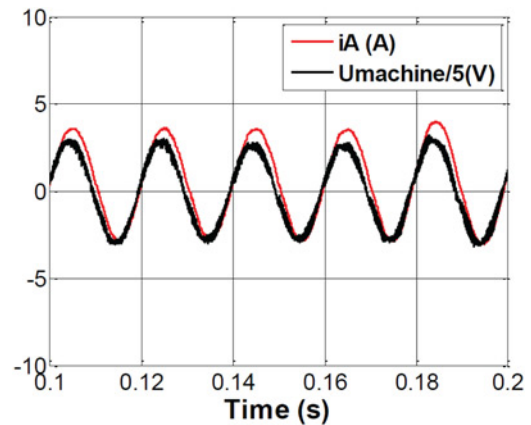
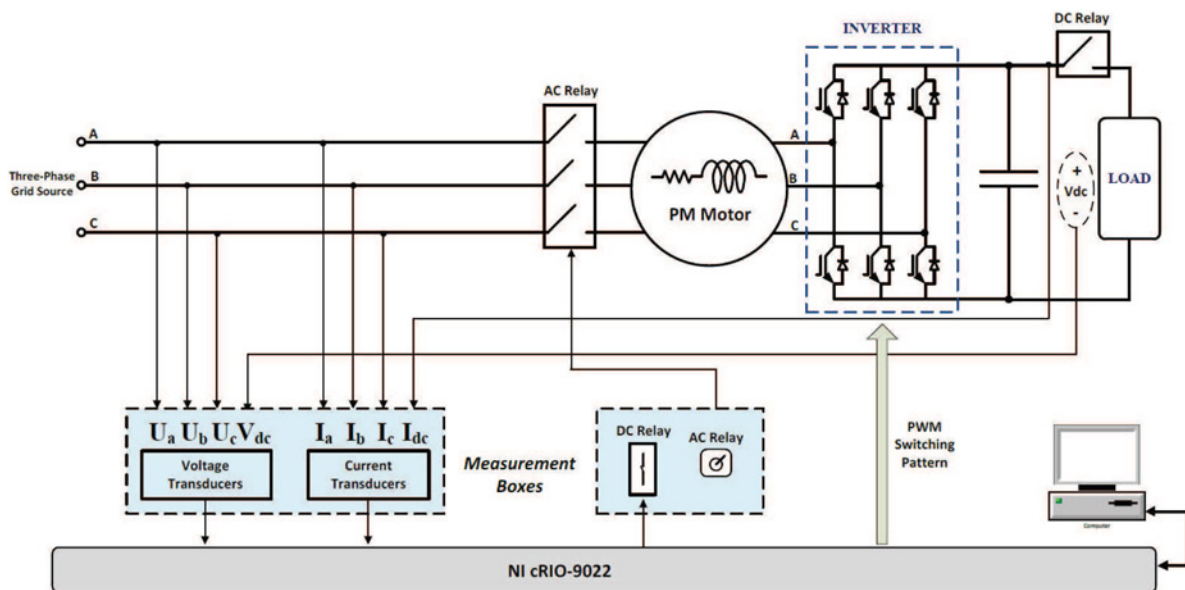
machine winding is measured and plotted in Fig. 16. Since the system is controlled during charging, the voltage drop in the machine remained sinusoidal. The voltage in the windings of the machine also remains in phase with the current of the corresponding phases that means that the control is acting to keep the power factor in the unity in the total system and also inside the motor.

In this setup, the motor is supplied by its rated current and no audible noise is observed during the charge operation. The motor inductance is a constant value for a PMSM that is not a function of rotor position. This motor has a distributed windings with a more sinusoidal back electromotive force compared with the 20 kW PM motor. Hence, the space harmonics are smaller compared with the 20 kW motor. Consequently, it is possible to increase the charging power up to the rated value.

As mentioned earlier, the main challenge of using a motor as some inductors in battery charger circuit is developed torque in the motor during the charge operation. In addition, if the motor inductance is constant in any arbitrary rotor position, it will be easier to keep the developed torque close to zero. To reduce the harmonics, one can use the distributed windings to have waveforms closer to the sinusoidal shape. Practical results show that a PMSM with two identical three-phase windings has apparently better performance compared with an IPMSM with two sets of windings that are shifted in the stator periphery with a variable inductance and poor windings' magnetomotive force (mmf). The developed torque of a PMSM during the battery charging is lower than that of an IPM motor. It is recommended to use a motor with a distributed windings to have a more sinusoidal

**Fig. 15** Measurement: the line phase A voltage and current for the 1 kW setup

mmf. The audible noise and the motor vibration are main limitations of the proposed system. One can optimise the system

**Fig. 16** Measurement: motor phase A voltage and current for the 1 kW setup**Fig. 14** main diagram of the experimental system using a CompactRIO platform

according to the above recommendations to achieve a higher-power level of charging.

6 Conclusion

An integrated motor drive and non-isolated battery charger based on a split-phase PM motor is presented and explained for the grid-connected vehicles. A switching relay is used to reconfigure the traction circuit to a three-phase Boost battery charger by changing the motor windings. The main idea is to insure standstill operation of the motor while charging. The circuit diagram, the practical realisation and the theoretical background of the operation is explained. Moreover, simulation and practical results are provided to verify the proposed system in charging mode. Two different experimental systems have been practically tested: one with a 20 kW split-phase IPMSM with a windings' phase-shift of $\pi/6$ degree and another one with a 1 kW split-phase PMSM with two identical sets of three-phase windings. As is shown by the simulation and practical results, the PMSM has a better performance in terms of the charging power and audible noise that is because of a more sinusoidal windings distribution and a constant motor inductance.

7 Acknowledgments

The authors would like to thank Isabel Serrano and Alvaro Bermejo, master students at Chalmers University of Technology, for helping with the experimental measurements. The project is financially supported by the Swedish Hybrid Vehicle Center (SHC) and Division of Electric Power Engineering of Chalmers University of Technology, Sweden.

8 References

- [1] Haghbin S.: 'Integrated motor drives and battery chargers for electric or plug-in hybrid electric vehicles'. PhD thesis, Chalmers University of Technology, 2013
- [2] Haghbin S., Lundmark S., Alakula M., Carlson O.: 'Grid-connected integrated battery chargers in vehicle applications: review and new solution', *IEEE Trans. Ind. Electron.*, 2013, **60**, (2), pp. 459–473
- [3] Yilmaz M., Krein P.: 'Review of battery charger topologies, charging power levels, and infrastructure for plug-in electric and hybrid vehicles', *IEEE Trans. Power Electron.* 2013, **28**, (5), pp. 2151–2169
- [4] Cocconi A.G.: 'Combined motor drive and battery recharge system'. US Patent no. 5,341,075, 23 August 1994
- [5] Rippel W.E.: 'Integrated traction inverter and battery charger apparatus'. US Patent no. 4,920,475, 24 April 1990
- [6] Rippel W.E.: 'Integrated motor drive and recharge system'. US Patent no. 5,099,186, 24 March 1992
- [7] De Sousa L., Silvestre B., Bouchez B.: 'A combined multiphase electric drive and fast battery charger for electric vehicles'. IEEE Vehicle Power and Propulsion Conf. (VPPC) Proc. 2010, France, October 2010
- [8] Bruyère A., De Sousa L., Bouchez B., Sandulescu P., Kestelyn X., Semail E.: 'A multiphase traction/fast-battery-charger drive for electric or plug-in hybrid vehicles'. IEEE Vehicle Power and Propulsion Conf. (VPPC) Proc. 2010, France, October 2010
- [9] Lacroix S., Laboure E., Hilairet M.: 'An integrated fast battery charger for electric vehicle'. IEEE Vehicle Power and Propulsion Conf. (VPPC) Proc. 2010, France, October 2010
- [10] Solero L.: 'Nonconventional on-board charger for electric vehicle propulsion batteries', *IEEE Trans. Veh. Technol.*, 2001, **50**, (1), pp. 144–149
- [11] Lee S.J., Sul S.K.: 'An integral battery charger for 4 wheel drive electric vehicle'. Industry Applications Society Annual Meeting, 1994., Conf. Record of the 1994 IEEE, October 1994, vol. 1, pp. 448–452
- [12] Haghbin S., Lundmark S., Alakula M., Carlson O.: 'An isolated high-power integrated charger in electrified-vehicle applications', *IEEE Trans. Veh. Technol.*, 2011, **60**, (9), pp. 4115–4126
- [13] Haghbin S., Khan K., Zhao S., Alakula M., Lundmark S., Carlson O.: 'An integrated 20-kw motor drive and isolated battery charger for plug-in vehicles', *IEEE Trans. Power Electron.*, 2013, **28**, (8), pp. 4013–4029
- [14] Lacressonniere F., Cassoret B.: 'Converter used as a battery charger and a motor speed controller in an industrial truck'. 2005 European Conf. Power Electronics and Applications, 2005
- [15] Haghbin S., Guillen I.: 'Integrated motor drive and non-isolated battery charger based on the torque cancellation in the motor'. 2013 IEEE Tenth Int. Conf. Power Electronics and Drive Systems (PEDS), April 2013, pp. 824–829
- [16] Estima J., Marques Cardoso A.: 'Efficiency analysis of drive train topologies applied to electric/hybrid vehicles', *IEEE Trans. Veh. Technol.*, 2012, **61**, (3), pp. 1021–1031
- [17] *Electromagnetic compatibility – Part 3-4: Limits – Limitation of emission of harmonic currents in low-voltage power supply systems for equipment with rated current greater than 16 A*, IEC 61000-3-4 Standard, First edition, 1998
- [18] Singh B., Singh B., Chandra A., Al-Haddad K., Pandey A., Kothari D.: 'A review of single-phase improved power quality ac-dc converters', *IEEE Trans. Ind. Electron.*, 2003, **50**, (5), pp. 962–981
- [19] Singh B., Singh B., Chandra A., Al-Haddad K., Pandey A., Kothari D.: 'A review of three-phase improved power quality ac-dc converters', *IEEE Trans. Ind. Electron.*, 2004, **51**, (3), pp. 641–660
- [20] Malinowski M.: 'Sensorless control strategies for three-phase pwm rectifiers'. PhD dissertation, Faculty of Electrical Engineering, Institute of Control and Industrial Electronics, Warsaw University of Technology, 2001
- [21] Lechat Sanjuan S.: 'Voltage oriented control of three-phase boost PWM converters'. Master thesis, Chalmers University of Technology, 2010
- [22] Mandiola J., Carmona D., Haghbin S., Abdulahovic T., Ellsen M.: 'An FPGA implementation of a voltage-oriented controlled three-phase PWM boost rectifier'. Electrical Systems for Aircraft, Railway and Ship Propulsion (ESARS), 2012, October 2012, pp. 1–6
- [23] Mohan N., Undeland M.T., Robbins W.P.: 'Power electronics: converters, applications, and design' (John Wiley and Sons, 1995)